

## REPORT DOCUMENTATION PAGE

Form Approved  
OMB No. 0704-0188

1. AGENCY USE ONLY (Leave blank)

2. REPORT DATE  
June 1, 1995

3. REPORT TYPE AND DATES COVERED  
Tech Rpt. # 23

## 4. TITLE AND SUBTITLE

Crystal Structure and Magnetic Susceptibility  
of  $\text{Ce}_8\text{Pd}_{24}\text{Sb}$ 

## 5. FUNDING NUMBERS

N00014-93-1-0904

Dr. John Pazik

R&amp;T: 3134037ess08

## 6. AUTHOR(S)

Robert A. Gordon and Francis J. DiSalvo

## 7. PERFORMING ORGANIZATION NAME(S) AND ADDRESS(ES)

Department of Chemistry  
Cornell University  
Ithaca, NY 14853-13018. PERFORMING ORGANIZATION  
REPORT NUMBER

## 9. SPONSORING/MONITORING AGENCY NAME(S) AND ADDRESS(ES)

Office of Naval Research  
Chemistry Program  
800 N. Quincy St.  
Alexandria, VA 2221710. SPONSORING/MONITORING  
AGENCY REPORT NUMBER

## 11. SUPPLEMENTARY NOTES

## 12a. DISTRIBUTION/AVAILABILITY STATEMENT

This document has been approved for public  
release and sale; its distribution is  
unlimited

## 12b. DISTRIBUTION CODE

## 13. ABSTRACT (Maximum 200 words)

The ternary compound  $\text{Ce}_8\text{Pd}_{24}\text{Sb}$  is very close in composition to the intermediate valent binary  $\text{CePd}_3$ . A single crystal study yielded a cubic cell with  $a=8.461(1)\text{\AA}$ ,  $\text{Pm}3\text{m}$  symmetry with  $wR2=0.0412$  based on 1453 reflections (222 unique) and 16 parameters. This new structure type is composed of distorted perovskite and  $\text{Cu}_3\text{Au}$  subcells arranged with the perovskite-like units centered on the corners of the cube. Fitting the magnetic susceptibility data above 100K to a Curie-Weiss expression yielded a Weiss constant of  $-15(3)\text{K}$  (anti-ferromagnetic) and an effective high temperature moment per cerium of  $2.45(4)\mu_B$  indicating trivalent behavior of the cerium atoms. No ordering was observed above 3K.

DTIC QUALITY INSPECTED 3

## 14. SUBJECT TERMS

cerium intermetallic, crystal structure, magnetic  
susceptibility

## 15. NUMBER OF PAGES

20

## 16. PRICE CODE

17. SECURITY CLASSIFICATION  
OF REPORT

Unclassified

18. SECURITY CLASSIFICATION  
OF THIS PAGE

Unclassified

19. SECURITY CLASSIFICATION  
OF ABSTRACT

Unclassified

## 20. LIMITATION OF ABSTRACT

19950626 051

**OFFICE OF NAVAL RESEARCH**

Grant or Contract N00014-93-1-0904

R&T Code 3134037ess08  
Scientific Officer: Dr. John Pazik

Technical Report No. 23

"Crystal Structure and Magnetic Susceptibility of  $\text{Ce}_8\text{Pd}_{24}\text{Sb}$ "

by

Robert A. Gordon and Francis J. DiSalvo

Submitted to

Z. Naturforsch. B

Cornell University  
Department of Chemistry  
Ithaca, NY 14853

June 1, 1995

Reproduction in whole or in part is permitted for any purpose  
of the United States Government

This document has been approved for public release  
and sale; its distribution is unlimited

# Crystal Structure and Magnetic Susceptibility of $\text{Ce}_8\text{Pd}_{24}\text{Sb}$

Robert. A. Gordon and Francis. J. DiSalvo<sup>1</sup>  
Department of Chemistry,  
Cornell University.  
Ithaca, NY 14853-1301

## Abstract

The ternary compound  $\text{Ce}_8\text{Pd}_{24}\text{Sb}$  is very close in composition to the intermediate valent binary  $\text{CePd}_3$ . A single crystal study yielded a cubic cell with  $a = 8.461(1)\text{\AA}$ ,  $\text{Pm}3\text{m}$  symmetry with  $wR2 = 0.0412$  based on 1453 reflections (222 unique) and 16 parameters. This new structure type is composed of distorted perovskite and  $\text{Cu}_3\text{Au}$  subcells arranged with the perovskite-like units centred on the corners of the cube. Fitting the magnetic susceptibility data above 100K to a Curie-Weiss expression yielded a Weiss constant of  $-15(3)\text{K}$  (anti-ferromagnetic) and an effective high temperature moment per cerium of  $2.45(4)\mu_B$  indicating tri-valent behavior of the cerium atoms. No ordering was observed above 3K.

Keywords: cerium intermetallic, crystal structure, magnetic susceptibility

---

<sup>1</sup> corresponding author

## 1. Introduction

Interaction between conduction electrons and the 4f electron on cerium can produce unusual electronic and magnetic effects such as magnetic ordering, heavy fermion behavior or intermediate valence (IV), where the 4f electron has significantly but not entirely delocalised [1-2]. A prototypical example of an intermediate valent material is  $\text{CePd}_3$ , where a strong Kondo interaction gives rise to broad maxima in the Seebeck co-efficient, resistivity and magnetic susceptibility [3-5]. When small elements such as B [3,6] or Si [3,5] were incorporated into  $\text{CePd}_3$ , in a perovskite-like fashion, the IV state was lost with heavy fermion or magnetic ordering [7] the end result. There is no published report of the incorporation of a larger p-block element into the  $\text{CePd}_3$  structure, until now.

We recently began exploring the Pd-rich region of the Ce-Pd-Sb phase diagram to see if new materials could be found which exhibit intermediate valent or heavy fermion behavior. We recently reported the anti-ferromagnet  $\text{Ce}_3\text{Pd}_6\text{Sb}_5$  [8]. Of the 3 other reported ternaries in this system,  $\text{CePdSb}$  [9],  $\text{CePd}_2\text{Sb}_2$  [10] and  $\text{CePdSb}_2$  [11], only  $\text{CePdSb}$  is reported to exhibit some Kondo behavior. In discovering the new phase  $\text{Ce}_8\text{Pd}_{24}\text{Sb}$ , we are presented with another opportunity to examine the sensitivity of the IV state with respect to small changes in local crystal and electronic structure.

## 2. Experimental

A sample of composition " $\text{Ce}_4\text{Pd}_{13}\text{Sb}_{3.03}$ " was prepared by arc-melting of the elements, all of at least 99.9% purity. The bead was turned over several times to ensure homogeneity. The

by	
Distribution/	
Availability Code	
Dist	Avail and/or Special
A-1	

final mass of the bead was consistent with losing 0.03 Sb (1% excess added to compensate for losses due to high Sb vapour pressure). This bead was subsequently placed in a vitreous carbon crucible (EMC Industries, type GAZ-02) and sealed under vacuum in a quartz tube. The tube was then placed within the coil of an induction furnace (Ameritherm Inc.) operating at 195kHz and subjected to the following heat treatment. The sample was first re-melted, then cooled to what appeared, by visual inspection, to be just below the melting point. The sample was then annealed at this point, which, by optical pyrometry, was at a temperature of 1100°C, for 20 hours before being allowed to cool to room temperature. The bead was removed from the tube and cooled to 77K in the hopes that the hard bead would be more brittle at liquid nitrogen temperature. The bead was broken apart under liquid nitrogen in an alumina mortar. After the first break, it became apparent that a single crystalline region approximately 1.5mm thick was present at the bottom of the bead. Further breaks enabled the isolation of both single crystals and multi-crystalline fragments. Inspection of the vitreous carbon crucible under a 40x microscope revealed no evidence of attack of the crucible. The crystals isolated are air-stable and jet black in colour with a mirror-like finish. Following the single crystal study, a sample of the title composition was prepared by arc-melting as above, placed in a section of tantalum tubing and sealed under vacuum in quartz. This bead was annealed for 2 weeks at 900°C.

Precession photographs of a single crystal needle mounted on a glass fibre were taken using an Enraf-Nonius Diffractis 601 and zirconium-filtered molybdenum  $K\alpha$  ( $\lambda = 0.71073\text{\AA}$ ) radiation. Single crystal intensity data for this same crystal were collected on a Siemens P4 automatic 4-circle diffractometer using graphite monochromatized molybdenum  $K\alpha$  radiation and controlled by the XSCAnS program [12]. Powder diffraction data was collected on a SCINTAG

$\theta$ -2 $\theta$  Diffractometer using Cu  $K\alpha_1$  radiation. Powder diffraction data on the sample of composition  $\text{Ce}_8\text{Pd}_{24}\text{Sb}$  was analysed using the program TREOR [13] and the resulting cell parameters were refined by a least-squares technique. Using the LAZY-PULVERIX program [14], a theoretical pattern was calculated for comparison to the observed powder pattern. Magnetic measurements were performed by the Faraday technique on polycrystalline material from the sample prepared at the title stoichiometry. Magnetic susceptibility data was fit to a Curie-Weiss expression as described previously [15].

### 3. Results and Discussion

#### 3.1. Crystal Structure

Precession photographs revealed strong peaks that indicated a cubic cell with a lattice constant of 4.2Å but the presence of weak reflections corresponding to twice this lattice parameter indicated the existence of a cubic supercell. No systematic zeros were observed in the photographs, leading to possible space groups P23, Pm3, P432, P43m and Pm3m. Consideration of additional symmetry in the photographs suggested a Laue symmetry of m3m. The Laue subroutine of the XSCANS program also indicated m3m symmetry which excludes the first 2 possible space groups. Refinements were carried out in Pm3m (No. 221), which is also the symmetry of  $\text{CePd}_3$ . Crystallographic data and details of the data collection are summarised in Table 1.

The starting atomic parameters were deduced from an interpretation of direct methods [16] and the structure was then successfully refined using SHELXL-93 [17] with anisotropic displacement parameters for all atoms. Initially, only the Ce and Pd positions were determined, with the Sb position becoming apparent from the difference Fourier map. A final difference Fourier syntheses revealed no significant residual peaks (all between  $+1.29$  and  $-1.17 \text{ e}/\text{\AA}^3$ ). The refined atomic parameters and the interatomic distances are listed in Tables 2 and 3. The lattice parameter obtained from a least-squares refinement using all powder diffraction peaks is  $8.4445(8)\text{\AA}$ . The small difference between powder and single crystal cell size is presumably due to alignment discrepancies between the two diffractometers. A comparison of experimental and calculated powder intensities is given in Table 4.

The structure of  $\text{Ce}_8\text{Pd}_{24}\text{Sb}$  (fig. 1) is of a new type, being composed of distorted perovskite and  $\text{Cu}_3\text{Au}$  subcells. The large size of the Sb atom is presumed to be driving the distortion since only an expansion of the lattice has been observed when a small atom such as B occupies the body-centre interstitial site in  $\text{CePd}_3$  [3,5,6]. Figure 2a shows the distorted perovskite unit " $\text{CeSbPd}_3$ " with an adjoining distorted  $\text{Cu}_3\text{Au}$  unit. The  $\text{Cu}_3\text{Au}$  unit found at the centre of the unit cell (fig. 2b) is essentially an expanded  $\text{CePd}_3$  cell  $4.207(1)\text{\AA}$  on edge (versus  $4.126\text{\AA}$  in binary  $\text{CePd}_3$  [3]), which is comparable to what Kappler et al.[3] refer to as "magnetic  $\text{CePd}_3$ ".

It is evident from fig. 2a that the Sb atom has pushed the Pd(2) atoms outward from the face of the perovskite cell. A close Pd(2)-Sb distance of  $2.633(1)\text{\AA}$  indicates a strong interaction between these two types of atoms when compared to the sum of their covalent radii,  $2.68\text{\AA}$ . Such close Pd-Sb contact has also been observed in  $\text{Ce}_3\text{Pd}_6\text{Sb}_5$  ( $2.629\text{\AA}$ ) [8] and in  $\text{EuPd}_2\text{Sb}_2$

(2.601Å) [10]. All other near-neighbour distances are comparable or larger than the sum of the appropriate covalent radii. The Ce-Pd(1) and Ce-Pd(3) distances are both comparable to the Ce-Pd distance in CePd<sub>3</sub> (2.97Å) while the Ce-Pd(2) distance is some 2.5% larger due to the displacement of Pd(2) from the face of the perovskite sub-cell. The Ce-Ce distance is also larger, being 4.207Å between nearest cerium atoms within the cell and 4.254Å between adjacent cells which are 2-3% increases over that in CePd<sub>3</sub> (4.126Å[3]). These Ce-Ce distances are comparable to the limiting cell size when B, Be, Si or Ge [3] are incorporated into the centre of a CePd<sub>3</sub> cell. It is also interesting to note that, while in CePd<sub>3</sub> all Pd-Pd near-neighbour distances are 2.97Å, in Ce<sub>8</sub>Pd<sub>24</sub>Sb, the Pd(2)-Pd(3) and Pd(3)-Pd(3) distances are significantly shortened to 2.765(1)Å and 2.791Å respectively. Both of these distances are comparable to the Pd-Pd distance in palladium metal (2.751Å) [18]. Overall, the structure of Ce<sub>8</sub>Pd<sub>24</sub>Sb could be viewed as a perturbation on CePd<sub>3</sub>.

### 3.2. Magnetic Susceptibility

The inverse of the magnetic susceptibility from 3.0K to 320K is shown in figure 3. No ordering is observed down to 3K but analysis of the data from 100K - 320K indicates an anti-ferromagnetic Weiss constant of -15(3)K and an effective cerium moment of 2.45(4) $\mu_B$ . Deviations from Curie behavior below 100K may be due to crystal field splitting of the cerium 4f<sup>1</sup> level, resulting in some temperature dependence to the cerium moment. Additional changes in slope below 50K may indicate the onset of significant magnetic fluctuations. Since the Weiss constant derived from high temperature data is the result of both exchange and crystal field effects [15], it is not possible to simply extract the exchange energy. In contrast to CePd<sub>3</sub>, the



effective cerium moment in  $\text{Ce}_8\text{Pd}_{24}\text{Sb}$  is consistent with tri-valent behavior. No feature that could be associated with a strong Kondo interaction is apparent. In perturbing  $\text{CePd}_3$  by incorporating one antimony per 8  $\text{CePd}_3$  units, with the accompanying small distortions, the intermediate valent state is lost.

#### 4. Conclusions

We have prepared and isolated crystals of a new ternary close in composition to the intermediate valent material  $\text{CePd}_3$ . This new ternary,  $\text{Ce}_8\text{Pd}_{24}\text{Sb}$ , is a cubic compound composed of expanded  $\text{CePd}_3$  units and distorted " $\text{CePd}_3$ " and perovskite " $\text{CeSbPd}_3$ " units. Magnetic measurements indicate an effective moment of  $2.45(4)\mu_B$  per cerium with no apparent magnetic order above 3K. Substitution of other large elements of the P-block is underway.

#### 5. Acknowledgements

We would like to acknowledge the support of the Office of Naval Research. We would also like to thank R.L.Gitzendanner and S.S.Trail for assistance with the precession work and Dr. E. Lobkovsky for assistance with the single crystal data collection. We appreciate discussions with Dr. H. Yamane and Dr. N.E. Brese concerning the solving of crystal structures using SHELX-93.

## 6. References

1. F. Steglich, C. Geibel, K. Gloos, G. Olesch, C. Schank, C. Wassilew, A. Loidl, A. Krimmel and G.R. Stewart, *J. Low Temp. Physics* **95**(1/2), 3 (1994).
2. M. Loewenhaupt and K.H. Fischer, in: *Handbook on the Chemistry and Physics of Rare Earths*, eds. K.A. Gschneider Jr. and L. Eyring, Chapter 105, Elsevier Science Publishers B.V., 1993.
3. J.P. Kappler, M.J. Besnus, P. Lehmann, A. Meyer and J. Sereni, *J. Less-Common Met.*, **111**, 261 (1985).
4. H. Sthioul, D. Jaccard and J. Sierro, in: *Valence Instabilities*, eds. P. Wachter and H. Boppart, p443, North-Holland Publishing Company, 1982.
5. S.K. Malik, R. Vijayaraghavan, E.B. Boltich, R.S. Craig and W.E. Wallace, *Solid State Comm.*, **43**(4), 243 (1982).
6. S.K. Dhar, S.K. Malik and R. Vijayaraghavan, *Mat. Res. Bull.*, **16**, 1557 (1981).
7. G. Nieva, J.G. Sereni and J.P. Kappler, *Physica Scripta*, **35**, 201-203 (1987).
8. R.A. Gordon, F.J. DiSalvo and R. Pöttgen, *J. Alloys Compounds*, accepted.
9. S.K. Malik and D.T. Adroja, *Phys. Rev. B*, **43**(7), 6295 (1991).
10. W.K. Hofmann and W. Jeitschko, *Monatshefte für Chemie*, **116**, 569 (1985).
11. O. Sologub, K. Hiebl, P. Rogl, H. Noël and O. Bodak, *J. Alloys Compounds*, **210**, 153 (1994).
12. XSCANS 2.0 Data Collection Package, copyright 1993, 1994, Siemens Industrial Automation Inc.
13. P.E. Werner, L. Eriksson and M. Westdahl, *J. Appl. Crystallogr.*, **18**, 367 (1985).

14. K. Yvon, W. Jeitschko and E. Parthé, *J. Appl. Crystallogr.*, **10**, 73 (1977).
15. R.A. Gordon, Y. Ijiri, C.M. Spencer and F.J. DiSalvo. *J. Alloys Compounds*, in press.
16. G.M. Sheldrick, SHELX-86, Program for the Solution of Crystal Structures, University of Göttingen, Germany, 1986.
17. G.M. Sheldrick, SHELX-93, Program for Crystal Structure Refinement, University of Göttingen, Germany, 1993.
18. J. Donohue, *The Structures of the Elements*, Wiley, New York (1974).
19. Structural figures were generated using ATOMS 3.1 ( $\beta 2$ ) for Windows, copyright 1994, E. Dowty.

Table 1. Crystal data and structure refinement for Ce<sub>8</sub>Pd<sub>24</sub>Sb.

Empirical formula	Ce <sub>8</sub> Pd <sub>24</sub> Sb
Formula weight	3796.31 g/mol
Temperature	293(2) K
Wavelengths	Mo K $\alpha$
Crystal system	cubic
Space group	Pm $\bar{3}$ m (No. 221)
Unit cell dimensions	$a = 8.461(1) \text{ \AA}$ $V = 605.71(2) \text{ \AA}^3$
Formula units per cell	$Z = 1$
Calculated density	10.408 g/cm <sup>3</sup>
Crystal size	18 x 38 x 232 $\mu\text{m}^3$
Absorption correction	from $\psi$ -scan data
Absorption coefficient	33.03 mm <sup>-1</sup>
F(000)	1619
$\theta$ range for data collection	3° to 60°
Scan mode	$\omega / \theta$
Range in $hkl$	$-1 \leq h, k, l \leq 11$
Total no. reflections	1453
Independent reflections	222 ( $R_{\text{int}} = 0.0548$ )
Refinement method	Full-matrix least-squares on $F^2$
Data/restraints/parameters	222 / 0 / 16
Goodness-of-fit on $F^2$	0.959
Final R indices [ $I > 2\sigma(I)$ ]	$R1 = 0.0170$ , $wR2 = 0.0412$
R indices (all data)	$R1 = 0.0216$ , $wR2 = 0.0412$
Extinction coefficient	0.00648(1)
Largest diff. peak and hole	1.29 and -1.17 $e^-/\text{\AA}^3$

Table 2. Atomic co-ordinates and isotropic displacement parameters (in pm<sup>2</sup>) for Ce<sub>8</sub>Pd<sub>24</sub>Sb.

Atom	Wyckoff site	x	y	z	U <sub>eq</sub> <sup>a)</sup>
Ce1	8g	0.25140(3)	0.25140(3)	0.25140(3)	82(2)
Pd1	12h	0.26675(7)	1/2	0	101(2)
Pd2	6e	0.31118(11)	0	0	128(2)
Pd3	6f	0.25552(8)	1/2	1/2	92(2)
Sb1	1a	0	0	0	194(4)

<sup>a)</sup> U<sub>eq</sub> is defined as one third of the trace of the orthogonalized  $U_{ij}$  tensor.

Table 3. Interatomic distances (Å) in the structure of  $\text{Ce}_8\text{Pd}_{24}\text{Sb}$ . All distances less than 4.5 Å are shown. Standard deviations are typically 0.001 Å or less.

Ce1:	3 Pd1 2.975	Pd1:	4 Pd1 2.925	Pd3:	2 Pd2 2.765
	6 Pd3 2.994		4 Pd3 2.927		2 Pd3 2.791
	3 Pd2 3.050		4 Ce1 2.975		2 Pd1 2.927
	1 Sb1 3.684		1 Pd1 4.137		4 Ce1 2.994
	3 Ce1 4.207		4 Pd3 4.232		2 Pd3 3.192
	3 Ce1 4.254				1 Pd3 3.947
		Pd2:	1 Sb1 2.633		2 Pd1 4.232
Sb1:	6 Pd2 2.633		4 Pd3 2.765		
	8 Ce1 3.684		4 Ce1 3.050		
			1 Pd2 3.195		
			4 Pd2 3.724		
			4 Pd3 4.247		

Table 4. Comparison of observed and calculated powder diffraction intensities for  $\text{Ce}_8\text{Pd}_{24}\text{Sb}$ .

h k l	$d_{\text{obs.}}(\text{\AA})$	$d_{\text{calc.}}(\text{\AA})$	$I_{\text{obs.}}(\%)$	$I_{\text{calc.}}(\%)$
2 2 0	2.9844	2.9858	7	4.7
3 0 0	2.8139	2.8150	3	2.6
2 2 1		2.8150		0.4
3 1 0	2.6690	2.6705	1	1.7
2 2 2	2.4369	2.4379	100	100
3 2 0	2.3404	2.3422	7	6.3
3 2 1	2.2568	2.2570	4	3.3
4 0 0	2.1106	2.1112	48	55
4 1 0		2.0482		0.9
3 2 2	2.0474	2.0482	8	6.3
3 3 0	1.9899	1.9905	2	1.7
4 1 1		1.9905		0.6
4 2 0	1.8885	1.8884	1	0.9
3 3 2	1.8007	1.8005	2	3.0
4 3 2	1.5677	1.5682	1	1.2
5 2 0		1.5682		0.4
4 4 0	1.4927	1.4929	40	31
5 2 2		1.4701		0.4
4 4 1	1.4696	1.4701	1	1.0
6 0 0		1.4075		0.2
4 4 2	1.4079	1.4075	1	1.3
6 2 0	1.3347	1.3353	2	3.0
5 4 0	1.3185	1.3189	2	1.3
6 2 1		1.3189		1.2
4 4 3		1.3189		0.3
6 2 2	1.2727	1.2731	27	30
6 3 0	1.2584	1.2589	3	2.2
5 4 2		1.2589		1.2
4 4 4	1.2186	1.2189	9	9.3
6 3 2	1.2063	1.2064	3	5.0
7 0 0		1.2064		0.3

## Figure Captions

Fig. 1. Crystal structure of  $\text{Ce}_8\text{Pd}_{24}\text{Sb}$  [19]. Palladium to palladium connections are shown to emphasize distortions in the structure. In order of decreasing size, circles represent: Ce (white), Sb (black) and Pd (gray).

Fig. 2. Distorted (a) and undistorted (b) sub-cells of  $\text{Ce}_8\text{Pd}_{24}\text{Sb}$ . Atom designations are as indicated in Fig. 1.

Fig. 3. Inverse magnetic susceptibility as a function of temperature from 3K to 320K for  $\text{Ce}_8\text{Pd}_{24}\text{Sb}$ . Data from 3K to 50K is shown inset.



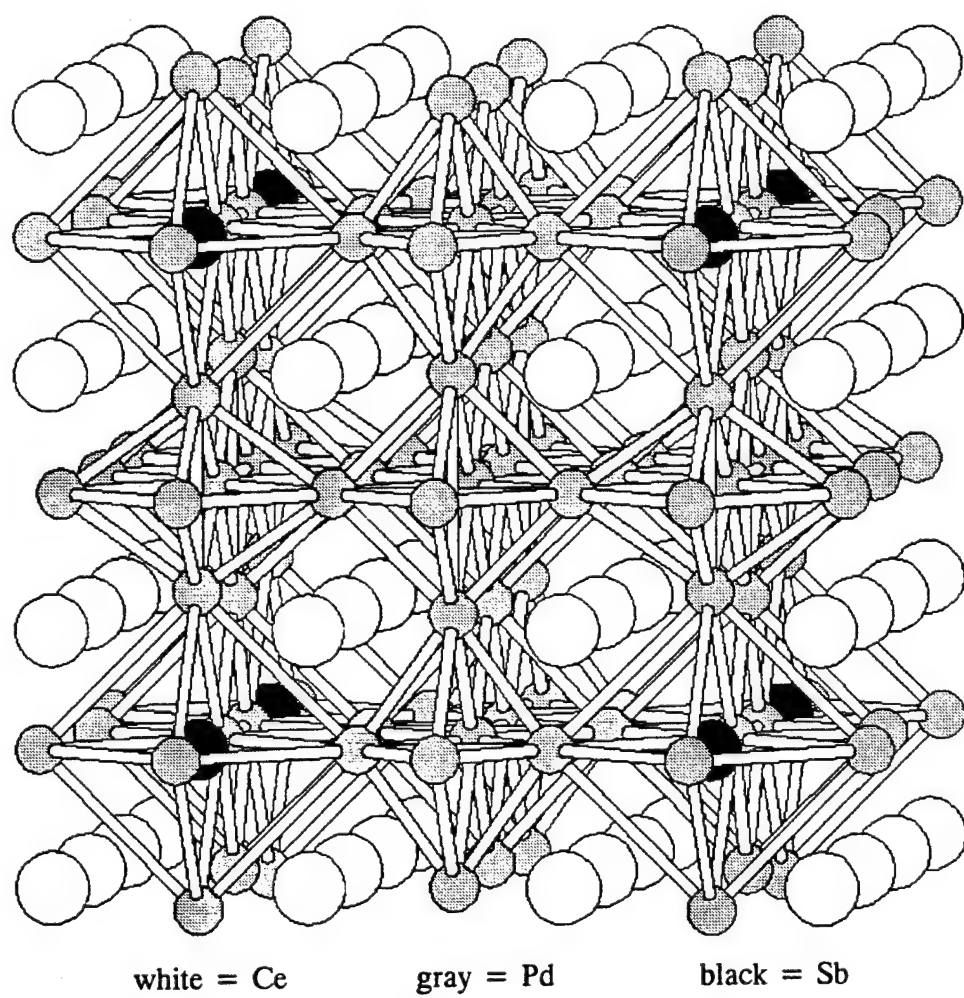


figure 1

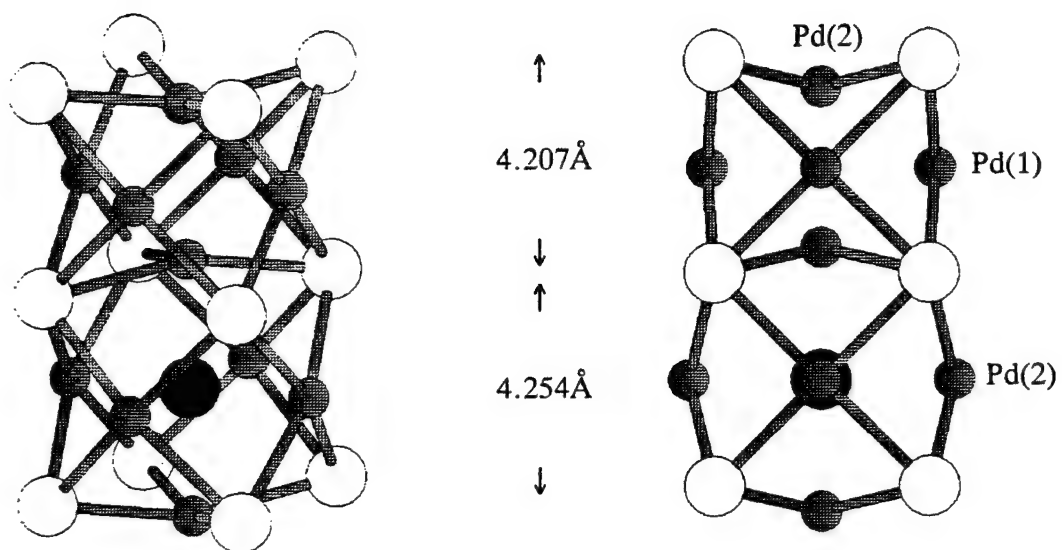


figure 2a

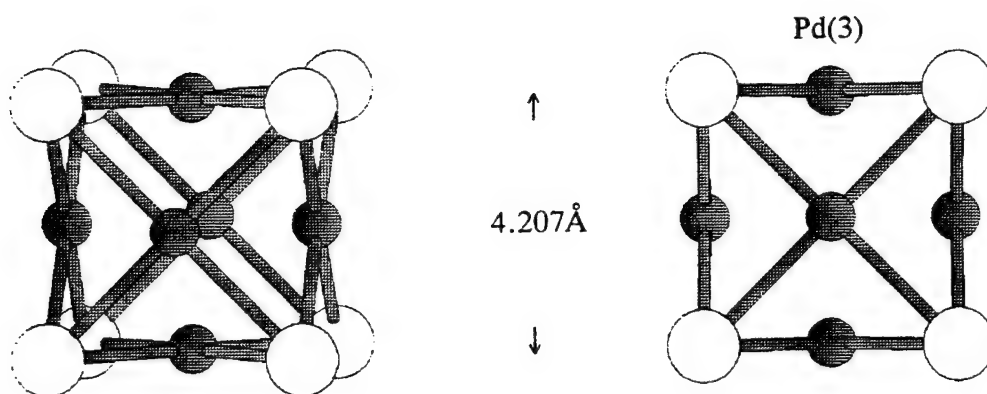


figure 2b

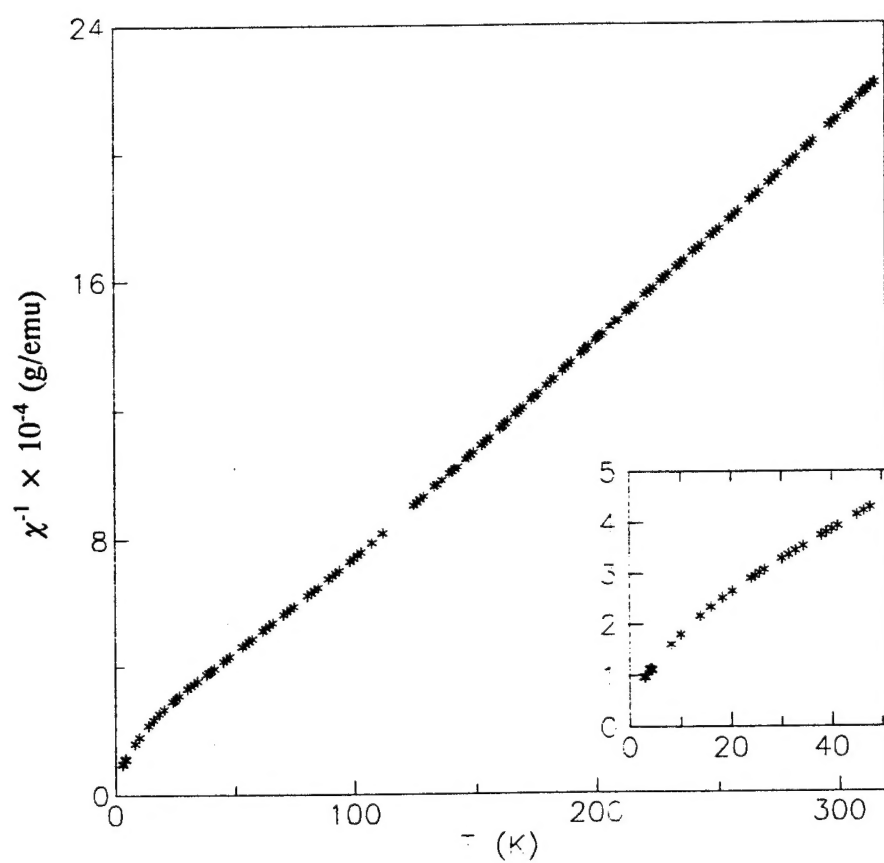


figure 3

Table 1. Observed and calculated structure factors for 1

h	k	l	10Fo	10Fc	10s	h	k	l	10Fo	10Fc	10s	h	k	l	10Fo	10Fc	10s	h	k	l	10Fo	10Fc	10s	h	k	l	10Fo	10Fc	10s
0	0	1	104	96	22	1	4	5	625	625	6	1	3	7	0	9	1	2	5	8	935	937	10	3	6	9	828	811	14
0	1	1	111	107	17	2	4	5	915	910	11	2	3	7	669	649	9	3	5	8	247	205	25	4	6	9	66	39	66
1	1	1	93	40	28	3	4	5	126	92	45	3	3	7	206	218	36	4	5	8	1445	1404	19	0	7	9	269	280	25
0	0	2	201	142	21	4	4	5	1551	1559	27	0	4	7	681	683	9	5	5	8	604	624	20	1	7	9	256	264	18
0	1	2	207	10		0	5	5	362	367	18	1	4	7	195	197	16	0	6	8	527	544	12	2	7	9	353	353	22
1	1	2	105	84	105	1	5	5	116	87	40	2	4	7	543	526	11	1	6	8	95	108	50	3	7	9	392	406	21
0	2	2	1786	1709	47	2	5	5	291	293	24	3	4	7	249	238	22	2	6	8	572	573	12	0	0	10	483	502	18
1	2	2	327	330	9	3	5	5	321	318	24	4	4	7	302	266	31	3	6	8	527	510	14	0	1	10	439	435	9
2	2	2	21085610852	106		4	5	5	695	651	15	0	5	7	0	38	1	4	6	8	862	847	12	1	1	10	79	93	79
0	0	3	1723	1674	42	5	5	5	137	108	136	1	5	7	193	177	17	5	6	8	433	440	19	0	2	10	1560	1581	19
0	1	3	712	713	6	0	0	6	632	631	12	2	5	7	37	61	37	6	6	8	923	921	18	1	2	10	445	445	9
1	1	3	362	366	6	0	1	6	763	774	7	3	5	7	68	33	67	0	7	8	243	264	25	2	2	10	4064	4188	60
0	2	3	1595	1581	19	1	1	6	508	518	5	4	5	7	319	310	20	1	7	8	274	269	15	0	3	10	1023	1029	11
1	2	3	836	830	8	0	2	6	2096	2111	24	5	5	7	0	119	1	2	7	8	152	138	44	1	3	10	429	435	10
2	2	3	1833	1847	30	1	2	6	811	813	7	0	6	7	1224	1249	15	3	7	8	96	69	95	2	3	10	1152	1144	18
0	3	3	1322	1346	19	2	2	6	6730	6677	60	1	6	7	509	505	8	4	7	8	47	26	46	3	3	10	733	744	17
1	3	3	667	681	7	0	3	6	1633	1664	22	2	6	7	1585	1553	16	5	7	8	362	351	23	0	4	10	121	130	58
2	3	3	1418	1401	27	1	3	6	989	1003	11	3	6	7	850	836	18	0	8	8	3322	3505	82	1	4	10	107	111	46
3	3	3	929	936	18	2	3	6	1830	1846	18	4	6	7	836	824	14	1	8	8	1005	1021	12	2	4	10	1103	1106	11
0	0	4	41086210815	148		3	3	6	1455	1415	20	5	6	7	357	329	20	2	8	8	1588	1625	24	3	4	10	684	671	12
0	1	4	687	692	6	0	4	6	130	97	35	6	6	7	1646	1651	39	3	8	8	344	350	33	4	4	10	264	235	40
1	1	4	580	593	4	1	4	6	252	239	11	0	7	7	239	243	33	0	0	9	613	601	16	0	5	10	20	36	20
0	2	4	930	928	11	2	4	6	1341	1369	16	1	7	7	366	365	15	0	1	9	262	247	13	1	5	10	43	35	43
1	2	4	429	435	5	3	4	6	1100	1052	12	2	7	7	263	255	33	1	1	9	525	536	7	2	5	10	102	45	102
2	2	4	776	756	14	4	4	6	562	541	18	3	7	7	189	169	52	0	2	9	120	141	47	3	5	10	277	278	28
0	3	4	751	766	8	0	5	6	141	120	31	4	7	7	57	16	56	1	2	9	300	296	11	4	5	10	203	222	39
1	3	4	111	108	21	1	5	6	266	257	11	5	7	7	270	290	45	2	2	9	311	309	24	0	6	10	1730	1778	24
2	3	4	722	729	7	2	5	6	119	30	47	6	7	7	457	473	28	0	3	9	592	593	12	1	6	10	695	706	9
3	3	4	707	689	13	3	5	6	712	680	10	0	0	8	6302	6168	109	1	3	9	697	703	7	2	6	10	3011	3121	48
0	4	4	8239	8245	116	4	5	6	268	254	22	0	1	8	756	751	7	2	3	9	647	658	11	0	0	11	624	635	19
1	4	4	1057	1071	13	5	5	6	118	74	117	1	1	8	538	532	6	3	3	9	874	856	16	0	1	11	243	241	18
2	4	4	1489	1455	20	0	6	6	2275	2325	32	0	2	8	1302	1291	11	0	4	9	864	858	10	1	1	11	544	543	9
3	4	4	191	177	38	1	6	6	1077	1088	12	1	2	8	602	614	6	1	4	9	75	42	74	0	2	11	443	444	14
4	4	4	6608	6554	118	2	6	6	4626	4649	63	2	2	8	118	100	69	2	4	9	438	441	14	1	2	11	180	186	22
0	0	5	1001	1016	26	3	6	6	1923	1895	40	0	3	8	213	191	20	3	4	9	311	288	20	2	2	11	834	850	15
0	1	5	278	277	8	4	6	6	1757	1698	29	1	3	8	114	82	28	4	4	9	1114	1073	17	0	3	11	107	79	106
1	1	5	0	46	1	5	6	6	425	419	24	2	3	8	150	158	35	0	5	9	123	121	55	1	3	11	362	364	12
0	2	5	538	535	8	6	6	6	3340	3342	85	3	3	8	344	328	23	1	5	9	493	497	9	2	3	11	80	97	80
1	2	5	141	150	16	0	0	7	1212	1210	31	0	4	8	5147	5110	88	2	5	9	143	135	49	3	3	11	207	195	51
2	2	5	585	595	12	0	1	7	157	139	17	1	4	8	1047	1024	9	3	5	9	665	648	12	0	4	11	327	332	20
0	3	5	319	317	11	1	1	7	261	262	10	2	4	8	1639	1596	17	4	5	9	126	125	78	1	4	11	433	436	11
1	3	5	325	335	8	0	2	7	1009	1027	17	3	4	8	183	160	32	5	5	9	462	465	26	2	4	11	164	157	46
2	3	5	439	429	11	1	2	7	222	230	12	4	4	8	4195	4250	65	0	6	9	237	245	26						
3	3	5	614	580	13	2	2	7	1394	1423	36	0	5	8	1226	1206	14	1	6	9	521	510	9						
0	4	5	1317	1320	16	0	3	7	611	605	11	1	5	8	586	589	7	2	6	9	109	87	109						

Table 2. Anisotropic displacement parameters (in  $\text{pm}^2$ ) for  $\text{Ce}_8\text{Pd}_{24}\text{Sb}$ .

ATOM	U11	U22	U33	U23	U13	U12
Ce(1)	82(2)	82(2)	82(2)	2(1)	2(1)	2(1)
Pd(1)	115(2)	82(3)	106(2)	0	0	0
Pd(2)	211(5)	87(2)	87(2)	0	0	0
Pd(3)	104(3)	87(2)	87(2)	0	0	0
Sb(1)	194(4)	194(4)	194(4)	0	0	0

Technical Report Distribution List

Dr. John C. Pazik (1)\*  
Physical S&T Division - ONR 331  
Office of Naval Research

800 N. Quincy St.  
Arlington, VA 22217-5660

Defense Technical Information  
Ctr (2)  
Building 5, Cameron Station  
Alexandria, VA 22314

Chemistry Division, Code 385  
NAWCWD - China Lake  
China Lake, CA 93555-6001

Dr. James S. Murday  
(1)  
Chemistry Division, NRL 6100  
Naval Research Laboratory  
Washington, DC 20375-5660

Dr. Peter Seligman (1)  
NCCOSC - NRAD  
San Diego, CA 92152-5000

Dr. Bernard E. Douda (1)  
Crane Division  
NAWC

Dr. John Fischer (1)

Crane, Indiana 47522-5000

\* Number of copies required